Spectroscopic Investigation of Tet Repressor Tryptophan-43 upon Specific and Nonspecific DNA Binding†

Claudia Peviani,‡ Wolfgang Hillen,§ Norbert Ettner,§,∥ Hans Lami,⊥ Silvia M. Doglia,‡ Etienne Piémont,⊥ Christine Ellouze,‡,# and Marie Chabbert*,⊥

Dipartimento di Fisica, Università degli Studi di Milano, Via Celoria 16, 20133 Milano, Italy, Consorzio Bioricerche, Polo Tecnologico di Milano Bicocca, Via Emanueli 15, 20126 Milano, Italy, Lehrstuhl für Mikrobiologie, Institut für Mikrobiologie und Biochemie der Friedrich-Alexander Universität Erlangen-Nürnberg, Staudtstrasse 5, 91058 Erlangen, FRG, and Laboratoire de Biophysique, Faculté de Pharmacie, Université Louis Pasteur de Strasbourg, CNRS URA 491, BP 24, 67401 Illkirch, France

Received February 6, 1995; Revised Manuscript Received June 1, 1995⊗

ABSTRACT: The F75 Tet repressor mutant (F75 TetR) contains a single tryptophan residue located at position 43 in the operator recognition α-helix. Previous studies [Hansen, D., & Hillen, W. (1987) *J. Biol. Chem. 262*, 12269−12274] have shown that the fluorescence intensity of this residue is dramatically reduced upon operator binding. In order to determine the origin of this quenching and the role of Trp-43 in the binding mechanism, we have investigated its fluorescence properties upon F75 TetR binding to a *tet* operator containing 76 bp DNA fragment (specific binding) and to sheared calf thymus DNA (nonspecific binding). Trp-43 steady-state fluorescence intensity was quenched by 72% upon specific binding and by 45% upon nonspecific binding. These fluorescence intensity decreases were not accounted for by similar decreases in the respective fluorescence lifetimes. The apparent quenching calculated from the average lifetimes was about 0.33 in both binding modes. This shows the presence of a static quenching process, clearly favored upon specific binding as compared to nonspecific binding. This is consistent with stacking interactions between Trp-43 and the DNA bases, as suggested by molecular graphics [Baumeister, R., Helbl, V., & Hillen, W. (1992) *J. Mol. Biol. 226*, 1257−1270]. The equilibrium constant between nonfluorescent and fluorescent tryptophan residues was 5 times higher upon binding to specific DNA than to nonspecific DNA. The preferential static quenching of Trp-43 in the specific complex suggests that stacking interactions might contribute to the specific binding mechanism. The spectroscopic parameters of *fluorescent* Trp-43 in both complexes differed mainly by a 6 nm shift in the emission maximum (339 nm for the specific complex, 345 nm for the nonspecific one), which might be related to the involvement of polar groups in hydrogen bonding in the specific complex. The dynamic quenching rate of Trp-43 by acrylamide decreased from 3.6×10^9 M^{-1} s^{-1} in free F75 TetR to 2.5×10^9 M^{-1} s^{-1} in both complexes, showing that *fluorescent* tryptophan was only partially buried upon DNA binding. The picosecond−subnanosecond rotational motion of Trp-43 ($S^2 \approx 0.6$) was not significantly altered upon binding, whereas the nanosecond segmental mobility decreased. Taken together, our results suggest that *fluorescent* Trp-43 residues, which are *not* involved in stacking interaction with DNA bases, would be in an environment less constrained and more accessible to solvent than in the molecular graphics model.

Regulation of gene expression by sequence-specific protein−DNA recognition plays a central role in all organisms. Sequence-specific recognition is realized by discrete DNA-binding domains, that can have several kinds of structures: helix−turn−helix, zinc finger, leucine zipper, or β-sheet [for a review, see Freemont et al. (1991)]. The most widely studied DNA-binding structural element is the α-helix−turn−α-helix motif, first discovered in prokaryotic repressors and activators. X-ray studies of repressor−operator crystals have established that amino acid side chains protude from the helix−turn−helix motif and interact with the edges of base pairs in the major groove by hydrogen bonds or van der Waals contacts (Harrison & Aggarwal, 1990; Steiz, 1990; Pabo & Sauer, 1992).

It has been suggested that stacking of tryptophan residues in DNA-binding proteins might be involved in base sequence discrimination (Rajeswary et al., 1987). However, to our knowledge, there is no example of stacking interactions between a Trp residue in a specific double-stranded DNA-binding protein and DNA base pairs. Most of the helix-turn-helix (HTH)[1] sequences known do not contain Trp residues. When they do, Trp is usually located at position 18 of the conventional HTH motif [e.g., P22 Cro, DicA, λ

† This work was supported by the Centre National de la Recherche Scientifique and the Université Louis Pasteur.

‡ Università degli Studi di Milano, and Polo Tecnologico di Milano Bicocca.

§ Institut für Mikrobiologie und Biochemie der Friedrich-Alexander Universität Erlangen-Nürnberg.

∥ Present address: Max-Planck-Institut für Biochemie, Abteilung Proteinchemie, 82152 Martinsried, FRG.

⊥ Université Louis Pasteur de Strasbourg.

Present address: Institut Curie, Groupe d'Etude Mutagénèse et Cancérogénèse, Université Paris-Sud, 91405 Orsay, France.

⊗ Abstract published in *Advance ACS Abstracts,* August 15, 1995.

[1] Abbreviations: HTH, helix−turn−helix; Tris-HCl, tris(hydroxymethyl)aminomethane hydrochloride; EDTA, ethylenediaminetetraacetic acid; βME, β-mercaptoethanol; bp, base pair; ct DNA, calf thymus DNA; sp DNA, specific DNA; nonsp DNA, nonspecific DNA.

0006-2960/95/0434-13007$09.00/0

Nul, and eukaryotic homeodomain proteins (Dodd & Egan, 1990)], where a hydrophobic residue is required and probably involved in the structural formation of the motif. One exception is Tet repressor (TetR) which controls transcription of the Tn*10*-encoded *tet* genes conferring resistance to tetracycline in Gram-negative bacteria (Beck et al., 1982; Bertrand et al., 1983; Hillen et al., 1984). X-ray studies confirmed the HTH structure of the operator-binding motif (Hinrichs et al., 1994). TetR Trp-43 is at position 17 of the conventional HTH motif, for which specific interaction with DNA bases is usually observed. Using single tryptophan mutants, Hansen and Hillen (1987) have shown that the steady-state fluorescence intensity of this Trp residue is strongly quenched upon operator binding, suggesting a tight contact with DNA. On the other hand, a "loss of contact" study in which Trp-43 was replaced by Ala led to a drastic decrease of binding to wild-type operator, but no base pair specific effects could be detected, suggesting that Trp-43 was involved in the structural architecture of the motif (Wissmann et al., 1991). Saturation mutagenesis of this residue has confirmed the need of an aromatic residue (Tyr or Phe) or of the imidazole ring system at that position for functional replacement mutants (albeit with reduced affinity) (Baumeister et al., 1992). Molecular graphics based on known repressor−operator structures indicated that Trp-43 could be located very close to the edges of base pairs 5 and 6, suggesting the possibility of stacking interactions with DNA bases (Baumeister et al., 1992).

The quenching observed by steady-state fluorescence (Hansen & Hillen, 1987) could be due either to a static quenching process or to additional deactivation pathways due to the vicinity of DNA as fluorescence resonance energy transfer or electron transfer from indole to DNA bases (Hélène & Lancelot, 1982). In order to determine the origin of the observed quenching and the possible involvement of stacking interactions in the specific binding mechanism of TetR, we have investigated the fluorescence properties of Trp-43 upon TetR binding to specific and nonspecific DNA, using the single Trp F75 TetR mutant (Hansen & Hillen, 1987). We show here that the main difference at the Trp-43 level between specific and nonspecific complexes lies in a different equilibrium constant between fluorescent and nonfluorescent tryptophans, suggesting that stacking interactions might play a role in the binding mechanism of TetR to its operator.

MATERIALS AND METHODS

Chemicals. All chemicals were of reagent grade or better. Sheared calf thymus DNA (ct DNA) was from Pharmacia and used without further purification. Its concentration was determined spectrophotometrically using an extinction coefficient of 13 100 M (bp)$^{-1}$ cm^{-1} at 260 nm. Ultrapure water (MilliQ instrument from Millipore Corp.) was used throughout the experiments. Except where otherwise noted, the experiments were carried out in 10 mM Tris-HCl, pH 8.0, 5 mM NaCl, 0.1 mM EDTA, and 10 mM β-mercaptoethanol. The temperature was 20 ± 1 °C.

F75 TetR Preparation. F75 TetR was purified as described elsewhere for wild-type TetR (Ettner & Jacob, 1993). This method led to a protein spectroscopically similar to that previously used (Chabbert et al., 1992). The purity of the protein, determined by scanning of gel bands, was more than 95%. The protein was stored at 4 °C as a precipitate in ammonium sulfate (60% saturation). Before measurements, an aliquot was dissolved in 20 mM Tris-HCl, pH 8.0, 200 mM NaCl, and 20 mM βME and buffer-exchanged using a PD10 column (Pharmacia). The extensive dialysis carried out previously (Chabbert et al., 1992) was avoided as this step led to a decrease in Trp-43 quantum yield. The concentration was determined spectrophotometrically using an extinction coefficient of 11 000 M (monomer)$^{-1}$ cm^{-1} at 280 nm.

Tet Operator 76 bp Fragment. The fragment of 76 bp used in this study ("specific DNA") contained the two operators $tetO_1$ and $tetO_2$, located approximately in the middle and separated by 30 bp between the centers of palindromic symmetry. Its sequence and preparation have been described elsewhere (Kleinschmidt et al., 1988). Operator concentrations were calculated on the basis of the number of operators and nucleotides per fragment.

Spectroscopic Methods. UV absorption spectra were recorded on a Cary 4 spectrophotometer. Steady-state fluorescence measurements were carried out with a MPF 66 spectrofluorometer (Perkin-Elmer). The excitation wavelength was 295 nm to excite specifically Trp fluorescence. Titrations were carried out by measuring the total fluorescence intensity under the fluorescence spectrum. Spectra were corrected for dilution, buffer fluorescence, and Raman scattering and, when DNA was present in the reaction mixture, for the screening effect due to the absorption of the nucleic acids. The absorbance of the sample at the excitation wavelength was measured after each DNA addition. The screening effect was determined experimentally, from an empirical correction curve obtained by recording the fluorescence intensity of a Trp solution as a function of DNA absorbance under conditions where Trp binding to DNA was not possible (0.5 M NaCl). Control measurements showed that the DNA *steady-state* fluorescence was negligible and needed no further corrections at the molar ratios of DNA to repressor used in this study.

The nonspecific association constant K_a was estimated from the half titration point of reverse titration curves of F75 TetR by ct DNA, using the noncooperative equation of McGhee and von Hippel (1974), with a site size N equal to the operator size (19 bp). Theorical fluorescence curves were generated as described elsewhere (Takahashi et al., 1990). For measurements carried out in the presence of nonspecific DNA, the amount of F75 TetR bound to nonspecific DNA was calculated from the equation of McGhee and von Hippel using $K_a = 1.4 \times 10^5$ M^{-1} and $N = 19$. This amount was within the experimental uncertainty of that determined experimentally by fluorescence. Nonspecific binding measurements were carried out under concentration conditions for which at least 90% of the protein was bound to ct DNA.

Acrylamide quenching measurements were carried out by adding aliquots of a concentrated stock solution of acrylamide to the sample. Fluorescence intensity, measured as the area under the spectrum for each acrylamide concentration, was corrected for dilution and screening effects due to the absorption of acrylamide at the excitation wavelength (295 nm). The reciprocal of the fluorescence intensity as a function of quencher concentration [Q] was linear in the concentration range investigated (0.2 M acrylamide) and could be fitted according to the classical Stern−Volmer equation (Eftink & Ghiron, 1976) using a least-squares

analysis procedure:

$$F_0/F = 1 + K_{SV}[Q] \quad (1)$$

in which F_0 is the initial fluorescence intensity, F the fluorescence intensity in the presence of an added quencher concentration [Q], and K_{SV} the Stern−Volmer constant.

Time-Resolved Measurements. Fluorescence lifetime measurements have been carried out with the pulse fluorometry technique, using a frequency-doubled rhodamine 6G dye laser, dumped and synchronously pumped by a mode-locked Argon laser (Spectra-Physics). The emission was detected at right angles to the excitation beam by a Hamamatsu R3809U microchannel plate, coupled to a Model 6954 pulse preamplifier (Phillips). A Schott WG320 filter was added on the emission side to eliminate residual light scattering. Since no color effect of the microchannel plate was observed, the instrument response function was recorded with a polished aluminium reflector. Its full width at half-maximum (FWHM) was about 70 ps. The excitation wavelength was 295 nm. The repetition rate was 800 kHz. The maximum data accumulation rate was 20 kHz. When necessary, neutral density filters were added in the excitation beam to reduce the intensity. The channel width was 53 ps and the number of channels used 512. The typical number of counts was 6×10^5.

Fluorescence Decay Data Analysis. The decay data were analyzed as sums of exponentials:

$$I(t) = \sum_i \alpha_i e^{-t/\tau_i} \quad (2a)$$

$$\text{with } \sum_i \alpha_i \tau_i = 1 \quad (2b)$$

by using an iterative reconvolution procedure based on the Marquardt algorithm. The weighting factors used in the χ^2 test were determined experimentally from a set of n decays. They correspond to the inverse of the diagonal elements of the sample covariance matrix determined from n decays (Lami & Piémont, 1992). The number of decays used ranged from 5 to 20. Rigorously, at least 20 decays should be necessary to estimate correctly the covariance matrix (Lami & Piémont, 1992). However, this considerably increased measurement times and, thus, UV irradiation of the sample. We observed a slow photodegradation of the Trp residue under UV irradiation. Thus, we had to reduce the number of the decays. Experimentally, we found that 5−10 decays were enough to estimate the covariance matrix. This led to an increase in the χ^2 value of about 0.3 as compared to that obtained from a set of 20 decays, but did not alter the decay parameters and prevented excessive photodegradation (typically 5% during a time-resolved emission spectrum).

The number of exponential components used in the fitting procedure was progressively increased until the fit was judged adequate from the χ^2 value and visual inspection of weighted residuals and autocorrelation factors. Four exponentials were required for an acceptable fit of the decay data of free F75 TetR. The fourth component was in the picosecond−subpicosecond range; it was not reproducible, and its weight was usually less that 0.5% of the total fluorescence intensity. This component was artifactual and could be related to the quantitation of the instrumental response function when the channel width is on the order of, or exceeds, the response function FWHM (Vix & Lami, 1995). Its weight markedly increased at 330 nm to take into account Raman scattering. In no case could it be related to the fluorescence decay of F75 TetR.

In the presence of DNA, four components were also required for an acceptable fit of the decay data. The amplitude of the picosecond component increased dramatically due to DNA background fluorescence. The DNA background fluorescence decay could be described by the sum of four exponential terms and was dominated by a picosecond component whose amplitude represented more than 95% of the total amplitude. We checked that this component was not due to the increased light scattering of the solution by comparison with the scattered light from a nondairy creamer suspended in distilled water. More probably, this ultrashort component is related to the fluorescence emission of the DNA bases (Daniels & Hauswirth, 1971; Ballini et al., 1983). Because of the jitter of the time-measuring device (Lami & Piémont, 1992), direct subtraction of the DNA fluorescence decay was not possible. Control experiments to estimate the DNA fluorescence contribution to the observed fluorescence decay of Trp-43 in the complexes were carried out by adding specific or nonspecific DNA to a F75 TetR solution in salt conditions (1.5 M NaCl) where no binding was possible (Kleinschmidt et al., 1988). At the molar ratios of DNA to repressor used in this study, the only significant change in the three components of F75 TetR fluorescence decay was an increase in the preexponential factor of the subnanosecond component on the red edge of the spectrum ($\lambda \geq 360$ nm). The lifetimes were not significantly altered. Corrections for the DNA contribution on the red edge of the spectrum could be carried out by estimating the relative weight of the DNA fluorescence and subtracting the corresponding preexponential factors (determined from DNA fluorescence decay analysis carried out with fixed lifetimes corresponding to those of F75 TetR). As the weight of the subnanosecond component in the total fluorescence decay was marginal (<5%), these corrections did not significantly alter the spectra associated with each component of the decay (see below) and their weight. We thus present uncorrected data. The average lifetime was defined by

$$\bar{\tau} = \sum_i \alpha_i \tau_i / \sum_i \alpha_i \quad (3)$$

Spectra associated with each component of the decay (DAS) were calculated from the steady-state fluorescence spectra and the multiexponential decay analysis data. The fluorescence associated with the component i at wavelength λ was calculated from (Wahl & Auchet, 1972)

$$F_i(\lambda) = F(\lambda)\alpha_i\tau_i / \sum_j \alpha_j \tau_j \quad (4)$$

The weight of component i, ω_i, was calculated from $S_i/\sum_j S_j$ where S_j was the area under the spectrum of component j. For nonspecific binding, these weights were corrected for the contribution of free F75 TetR fluorescence. The relative amplitude of component i, A_i, was calculated from

$$A_i = (\omega_i/\langle\tau_i\rangle)/(\sum_j \omega_j/\langle\tau_j\rangle) \quad (5)$$

Anisotropy Measurements. Steady-state anisotropy measurements were carried out on an SLM 8000 spectrofluorometer (T-format device), with the excitation and emission wavelengths set at 295 and 350 nm, respectively. Time-

resolved anisotropy measurements were carried out by using the device of the fluorescence decay measurements. The emission wavelength was 350 nm. The polarization of the emission beam was vertical. The polarization of the excitation beam could rotate by using a home-built device. To avoid polarization bias due to the different dead times of the vertical and horizontal excitation decays when they are alternatively recorded, the decays with vertical and horizontal excitation polarization, $I_v(t)$ and $I_h(t)$, were separately recorded. The total fluorescence intensity $I_t(t)$ was built from $I_v(t) + 2GI_h(t)$. The corrective factor G was equal to

$$G = [(1 - r)\int I_v(t)\,dt]/[(1 + 2r)\int I_h(t)\,dt] \quad (6)$$

The steady-state anisotropy r used for the corrective factor was measured by using the time-resolved device at very low counting frequency (<1 kHz) and correlated well with the steady-state anisotropy measurements carried out with the SLM 8000 spectrofluorometer.

The fluorescence anisotropy $r(t)$ was obtained by fitting the experimental $I_v(t)$ decay directly to the anisotropy-containing expression for this fluorescence component (Cross & Fleming, 1984). The $r(t)$ decay was fit as

$$r(t) = \sum_i r_i \exp(-t/\theta_i) + r_\infty \quad (7)$$

where r_i is the amplitude of the rotational correlation time θ_i and r_∞ the infinite time anisotropy. The parameters for the total fluorescence intensity decay used in the anisotropy decay fit were those obtained by the deconvolution of $I_v + 2GI_h$. They were within the experimental uncertainty of those obtained for the magic-angle decay data. The data could be adequately fit by two components as judged from the χ^2 values and the plots of the residuals. The three-component analysis did not converge. As for the decay measurements, the anisotropy decay measurements were repeated n times on the same sample (typically 10) to determine the sample covariance matrix and to analyze statistically the set of decay parameters obtained.

RESULTS

Steady-State Fluorescence Properties of F75 TetR upon DNA Binding. The F75 mutation did not significantly alter the association constant of about 5×10^{11} M^{-1} of Tet repressor for *tet* operator (Hansen & Hillen, 1987). In agreement with this very high value, upon titration of F75 TetR by the *tet* operator containing 76 bp fragment, the fluorescence intensity of Trp-43 decreased linearly with the *tet* operator concentration until a molar ratio of 0.96 ± 0.04 operator by repressor dimer was attained, and then reached a plateau corresponding to 28% of the initial fluorescence intensity (Figure 1a). This is consistent with the 1:1 stoichiometry of the Tet repressor–*tet* operator complex and clearly indicates that most of the residual fluorescence cannot be due to denatured protein unable to bind to the operator. To confirm this assumption and to check the possibility of fluorescent impurities, we further purified F75 TetR by FPLC on a monoQ column as previously described (Chabbert et al., 1992). Immediately after the chromatography, the protein sample was buffer-exchanged on a PD10 column, and binding to *tet* operator DNA was carried out in the presence of either 5 mM or 100 mM NaCl. We did not observe any change in the spectroscopic properties of this F75 TetR

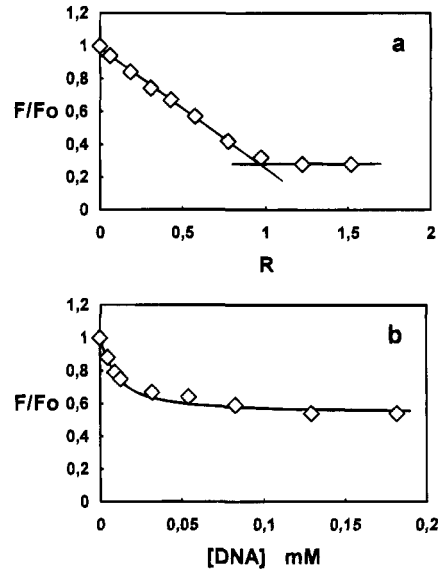

FIGURE 1: Titration of F75 TetR by the *tet* operator containing 76 bp fragment (a) and by sheared ct DNA (b). The buffer used was 10 mM Tris, pH 8.0, 5 mM NaCl, 10 mM βME, and 0.1 mM EDTA. F/F_0 represents the relative fluorescence intensity decrease. Specific binding measurements were carried out with a F75 TetR dimer concentration of 1 μM. R represents the molar ratio of the operator to repressor dimer. The straight lines in (a) represent the linear best fit of the data (up to $R = 0.8$) and the plateau reached. Nonspecific binding measurements were carried out with a F75 TetR dimer concentration of 0.17 μM. The data are plotted as a function of the total sheared calf thymus DNA concentration. The simulated curve in (b) was obtained with $K_a = 1.4 \times 10^5$ M^{-1} and $N = 19$.

preparation, either free or bound to the 76 bp operator fragment, as compared to those observed without the FPLC purification step. This clearly shows that the residual fluorescence is related to Trp-43 in F75 TetR bound to *tet* operator. Upon titration of F75 TetR by sheared ct DNA, the Trp-43 fluorescence intensity monotonically decreased and reached a plateau corresponding to 55% of the initial fluorescence intensity (Figure 1b). The apparent association constant of F75 TetR for nonspecific DNA was estimated to be 1.4×10^5 M^{-1} from the half titration point of the titration curve (see Materials and Methods). This value is similar to that determined for wild-type TetR in 10 mM NaCl (Kleinschmidt et al., 1988), and corroborates the assumption that the F75 mutation does not alter the affinity of TetR for DNA.

Figure 2 displays the fluorescence spectra of F75 TetR free and complexed to specific and nonspecific DNA, upon excitation at 295 nm. We checked that the spectra obtained at a higher excitation wavelength (e.g., 297 nm) were identical to those obtained at 295 nm, showing that Trp-43 was selectively excited, without contribution from tyrosine residues. The emission maximum of Trp-43 at low ionic concentration was 348 nm. The binding of F75 TetR to sheared calf thymus DNA induced a 3 nm shift in the emission maximum and that to the *tet* operator containing 76 bp fragment a 9 nm blue shift (Table 1). The addition of 100 mM NaCl did not significantly modify the characteristics of F75 TetR binding to the 76 bp fragment (Table 1), whereas no binding to nonspecific DNA could be observed at this ionic concentration, in agreement with the ionic strength dependence of wild-type TetR nonspecific binding (Kleinschimdt et al.,1988).

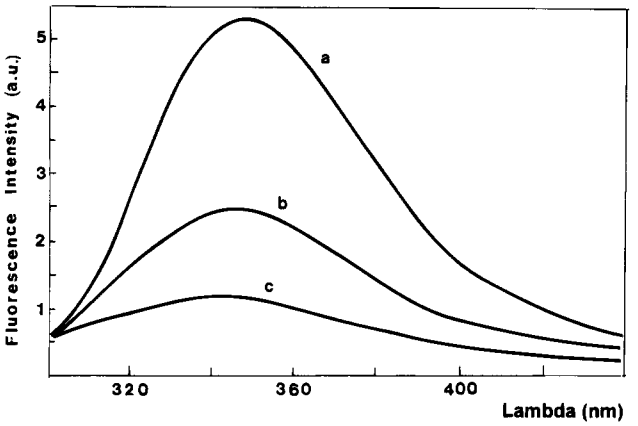

FIGURE 2: Steady-state fluorescence spectra of Trp-43 in F75 TetR free (a) and bound to sheared ct DNA (b) and to the *tet* operator containing 76 bp fragment (c). The excitation wavelength was 295 nm. The F75 TetR dimer concentration was 0.50 μM. When present, the concentration of the 76 bp fragment was 32 μM (bp), and that of ct DNA was 144 μM (bp). In the presence of nonspecific DNA, 95% of F75 TetR was bound to DNA. The spectra were corrected for the Raman contribution and for the screening effect of the DNA bases.

Excitation spectra of free and bound F75 TetR were monitored at an emission wavelength of 350 nm, where Trp-43 was selectively observed. Comparison of excitation spectra was not straightforward because of the screening effect due to nucleic acids. However, as the ionic concentration did not alter the excitation spectrum of free repressor, measurements were carried out by comparing excitation spectra of mixtures of repressor and DNA at low ionic concentration (bound state) and at high ionic concentration (unbound state). No change in the excitation spectrum of Trp-43 was observed upon F75 TetR binding to specific or nonspecific DNA (not shown).

Acrylamide fluorescence quenching measurements were carried out in an attempt to better characterize the environment of Trp-43 upon binding. Since complex formation with nonspecific DNA requires low ionic strength, use of ionic quenchers such as iodide was not possible. Moreover, a neutral quencher was highly preferable to avoid repulsion by the negative charges of DNA. The Stern–Volmer plots of the acrylamide quenching of Trp-43 in free or bound F75 TetR were linear (not shown) and thus could be fitted according to eq 1. The Stern–Volmer constants corresponding to the best fits are reported in Table 1. Using the average lifetime of the fluorescence decay at 350 nm (see below), the dynamic quenching rate defined as $k_q = K_{SV}/\bar{\tau}$ could be calculated. Upon complex formation, the dynamic quenching rate decreased by about 30% from 3.6×10^9 M^{-1} s^{-1} in free F75 TetR to 2.5×10^9 M^{-1} s^{-1} in both complexes, showing a reduced accessibility of Trp-43 to acrylamide upon binding. The rate constant for free F75 TetR is typical of a Trp residue exposed to the solvent (Eftink & Ghiron, 1976) and consistent with its position on the surface of the protein. In either complex, Trp-43 was only partially buried and had the same accessibility to solvent.

Time-Resolved Fluorescence. Table 2 reports the results of typical fluorescence decay multiexponential analysis of Trp-43 in F75 TetR free and complexed to either specific or nonspecific DNA. As detailed under Materials and Methods, the fluorescence decay of Trp-43, either in the absence or in the presence of DNA, could be described by the sum of four exponential terms. However, the fourth component, in the picosecond–subpicosecond range, was not related to the fluorescence decay of Trp-43, and is therefore excluded from data reported here. In a previous report (Chabbert et al., 1992), we described the fluorescence decay of Trp-43 in free TetR with two decay times. The difference to this report is related to the drastic improvement in data resolution due to a microchannel plate in this study as compared to a photomultiplier in the previous study. When the present data are analyzed with two components, the decay parameters are quite similar to those previously published, albeit with a very high χ^2 (>4). Due to the improved resolution of the device, the previously reported 1.3-ns component can now be resolved into two components. It is possible to estimate an apparent radiative decay rate from the ratio of the quantum yield to the average lifetime at 350 nm, 3.5 ns. Under the present experimental conditions, the quantum yield was 0.18 $\pm$ 0.01, which leads to a radiative decay rate of $(0.51 \pm 0.05) \times 10^9$ s^{-1}, consistent with that determined for *N*-acetyl-L-tryptophanamide in water (Werner & Forster, 1979).

The lifetimes of the three components that described the decay were marginally altered upon binding to either specific or nonspecific DNA (Table 2). The long lifetime decreased by less than 10% and the intermediate lifetime by about 25%, whereas the subnanosecond lifetime was not significantly altered. Despite the similarities in the lifetimes, major changes were observed in the preexponential factors of the shortest two components. The preexponential factor of the 2-ns component increased by more than 50% and that of the 0.3-ns component by more than 100%. The preexponential factor of the longest component was not significantly altered upon binding. The absence of a DNA contribution to the observed fluorescence decay was confirmed by the similarity in the fluorescence decay parameters of Trp-43 at two different molar ratios of DNA to repressor (Table 2). To examine the effect of ionic concentration, decay measurements were also carried out in the presence of 100 mM NaCl. The addition of 100 mM NaCl did not significantly alter the decay parameters of Trp-43 in F75 TetR either free or bound to the *tet* operator containing 76 bp fragment (Table 2), which echoes the similarity in the steady-state spectral features (Table 1).

Either in free F75 TetR or in both complexes, the three lifetimes showed only a slight variation with the emission wavelength. They averaged 6.2 $\pm$ 0.2 ns, 2.5 $\pm$ 0.3 ns, and 0.27 $\pm$ 0.03 ns in free F75 TetR, 6.0 $\pm$ 0.3 ns, 2.0 $\pm$ 0.1 ns, and 0.33 $\pm$ 0.06 ns for the specific complex, and 5.8 $\pm$ 0.2 ns, 1.9 $\pm$ 0.1 ns, and 0.26 $\pm$ 0.03 ns for the nonspecific complex. In either case, the preexponential factors of the longest component did not display significant wavelength dependence. For free F75 TetR, the preexponential factors of the 2.5-ns component markedly decreased from 0.14 at 320 nm to 0.08 at 380 nm and that of the 0.3-ns component from 0.10 to 0.04. In either complex, the preexponential factors of the 2-ns component decreased from 0.20 at 320 nm to 0.14 at 380 nm. The preexponential factors of the 0.3-ns component decreased from 0.19 at 320 nm to 0.13 at 360 nm and then slightly increased on the red edge of the spectra due to a contribution from DNA background fluorescence. Because of the marginal weight of this component in the total fluorescence decay, the contribution from DNA fluorescence to the subnanosecond component did not significantly alter the other two preexponential factors as defined by eq 2b.

Table 1: Spectroscopic Parameters of Trp-43 upon F75 TetR Binding to Specific or Nonspecific DNA[a]

conditions	F75 TetR	λ_M (nm)	F/F_0	K_{sv} (M^{-1})[d]	$\bar{\tau}$ (ns)[e]	k_q (M^{-1} s^{-1}) × 10^{-9}
5 mM NaCl	free	348 ± 1		12.6 ± 0.6	3.5 ± 0.2	3.6 ± 0.3
	+sp DNA	339 ± 1	0.28 ± 0.01[b]	5.8 ± 0.5	2.3 ± 0.1	2.5 ± 0.3
	+nonsp DNA	345 ± 1	0.55 ± 0.02[c]	6.1 ± 0.4	2.4 ± 0.1	2.5 ± 0.3
100 mM NaCl	free	349 ± 1			3.7 ± 0.2	
	+sp DNA	340 ± 1	0.28 ± 0.01[b]		2.5 ± 0.1	

[a] Measurements were carried out in a buffer containing 10 mM Tris, pH 8.0, 10 mM βME, 0.1 mM EDTA, and NaCl at the concentration indicated. The excitation wavelength was set at 295 nm. λ_M represents the wavelength of the fluorescence emission maximum; F_0 and F are the total fluorescence intensity of Trp-43 in free F75 TetR and in the complex with DNA; K_{sv} is the Stern−Volmer constant and k_q the dynamic quenching rate for acrylamide quenching. The average lifetime at 350 nm, τ, is defined by eq 3. The data represent the means (± standard errors) of at least three independent measurements except for acrylamide quenching data which correspond to the means of two independent measurements. [b] Measured as the plateau reached upon titration of F75 TetR by the *tet* operator containing 76 bp fragment at a dimer concentration of 1 μM. [c] Measured as the plateau reached upon titration of F75 TetR by ct DNA at a dimer concentration of 0.2 μM. [d] The F75 TetR dimer concentration was 0.5 μM. When present, the concentration of the 76 bp fragment was 32 μM (bp), and that of ct DNA was 144 μM (bp). Upon nonspecific binding, measurements were carried out with 95% of the repressor bound to DNA. [e] The F75 TetR dimer concentration ranged from 1.0 to 1.5 μM. When the *tet* operator containing 76 bp fragment was present, the molar ratio of operator to repressor dimer was 1.5. When sheared ct DNA was present, its concentration was such that 92 ± 2% of repressor was bound to DNA.

Table 2: Multiexponential Analysis of Typical Fluorescence Decays of Trp-43 at 350 nm[a]

conditions	F75 TetR	τ_1 (ns)	α_1	τ_2 (ns)	α_2	τ_3 (ns)	α_3	χ^2
5 mM NaCl	free[b]	6.3 ± 0.1	0.112 ± 0.005	2.6 ± 0.1	0.107 ± 0.005	0.27 ± 0.02	0.042 ± 0.004	1.3
	+sp DNA[b]	6.0 ± 0.1	0.105 ± 0.005	2.0 ± 0.1	0.169 ± 0.003	0.28 ± 0.02	0.127 ± 0.011	1.3
	+nonsp DNA[c]	5.8 ± 0.1	0.113 ± 0.002	2.0 ± 0.1	0.157 ± 0.003	0.26 ± 0.02	0.136 ± 0.006	1.4
	+nonsp DNA[d]	5.7 ± 0.1	0.114 ± 0.002	1.8 ± 0.1	0.172 ± 0.003	0.27 ± 0.02	0.142 ± 0.004	1.6
100 mM NaCl	free[b]	6.5 ± 0.1	0.104 ± 0.003	2.6 ± 0.1	0.122 ± 0.003	0.21 ± 0.02	0.052 ± 0.007	1.5
	+sp DNA[b]	6.0 ± 0.1	0.101 ± 0.004	2.0 ± 0.1	0.171 ± 0.004	0.28 ± 0.04	0.137 ± 0.011	1.3

[a] Measurements have been carried out as described under Materials and Methods, in a buffer containing 10 mM Tris, pH 8.0, 10 mM βME, 0.1 mM EDTA, and NaCl at the concentration indicated. The emission wavelength was 350 nm. Trp-43 fluorescence decays were analyzed as sums of four exponential components. The shortest component, in the picosecond time scale, is not related to Trp-43 fluorescence decay (see Materials and Methods) and is excluded from data presented here. The decay data correspond to the means (± standard errors) of at least 5 measurements on the same sample. [b] The F75 TetR dimer concentration was 1.0 μM (100 mM NaCl) or 1.4 μM (5 mM NaCl). When the *tet* operator containing 76 bp fragment was present, the molar ratio of operator to repressor dimer was 1.4. [c] The concentration of the F75 TetR dimer was 1.1 μM, and that of ct DNA was 96 μM (pb), which corresponds to 90% of protein bound to DNA. [d] The concentration of the F75 TetR dimer was 1.1 μM, and that of ct DNA was 143 μM (bp), which corresponds to 94% of protein bound to DNA.

The spectra associated with each component of the decay (DAS) could be calculated from eq 4 (Figure 3). Either in free F75 TetR or in the complexes, the fluorescence spectrum of Trp-43 was dominated by the long component whose emission maximum was similar to that of the steady-state spectrum. Its weight decreased from 75% of the total fluorescence intensity in free TetR to about 65% in both complexes. The weight of the intermediate component increased from 24% to about 30% upon binding. This component was about 5 nm blue-shifted as compared to the long component. The short-lived component was clearly blue-shifted (10−15 nm) and contributed only marginally to the fluorescence. However, its weight significantly increased from 1% to 3−4% upon binding.

Taken together, the fluorescence decay data are consistent with a general three-state model, in which the equilibrium between three "species" of fluorescent Trp residues, characterized by different decay rates, would be altered upon DNA binding. Under the assumption that these species do not interconvert on the fluorescence lifetime, the experimentally determined decay times correspond to the species lifetimes, and their spectra are determined by eq 4. With the additional hypothesis that these species have the same extinction coefficient and radiative decay rate, the ratio of their ground state concentrations corresponds to the relative amplitude of each decay component (eq 5). The relative concentration of the 6-ns species decreased from 0.47 in free F75 TetR to about 0.30 upon DNA binding, whereas that of the 0.3-ns species increased from 0.15 to about 0.30. The relative concentration of the 2-ns species, 0.38 in free F75 TetR, was not significantly altered upon binding.

Anisotropy Measurements. Table 3 summarizes the parameters describing the rotational mobility of Trp-43 in free or bound F75 TetR. Steady-state anisotropy measurements showed a slight increase in the anisotropy upon complex formation. However, we could estimate an average rotational correlation time ϕ using the Perrin equation (Lakowicz, 1983):

$$r/r_0 = 1 + \langle\tau\rangle/\phi \qquad (8)$$

where r_0 is the limit anisotropy and $\langle\tau\rangle$ is the mean lifetime, defined as $\langle\tau\rangle = (\sum_i \alpha_i\tau_i^2)/(\sum_i \alpha_i\tau_i)$. The limit anisotropy of Trp-43 is equal to 0.27 (Chabbert et al., 1992). The mean lifetime decreased from 5.1 ± 0.2 ns in free F75 TetR to 4.4 ± 0.2 ns in both complexes. The rotational correlation time of Trp-43 increased from 2.2 ns in free F75 TetR to about 3 ns in both complexes (Table 3), indicating a significant decrease in Trp-43 mobility.

Time-resolved fluorescence anisotropy measurements have been carried out to further characterize the rotational motion of Trp-43. In any case, the anisotropy decay showed the existence of motion with two clearly distinct time scales (Table 3). The shortest rotational correlation time, on the subnanosecond time scale, was attributed to fast wobbling of Trp-43. The longest one, on the nanosecond time scale, probably corresponded to segmental motion of a larger part of the protein. The infinite time anisotropies were not zero,

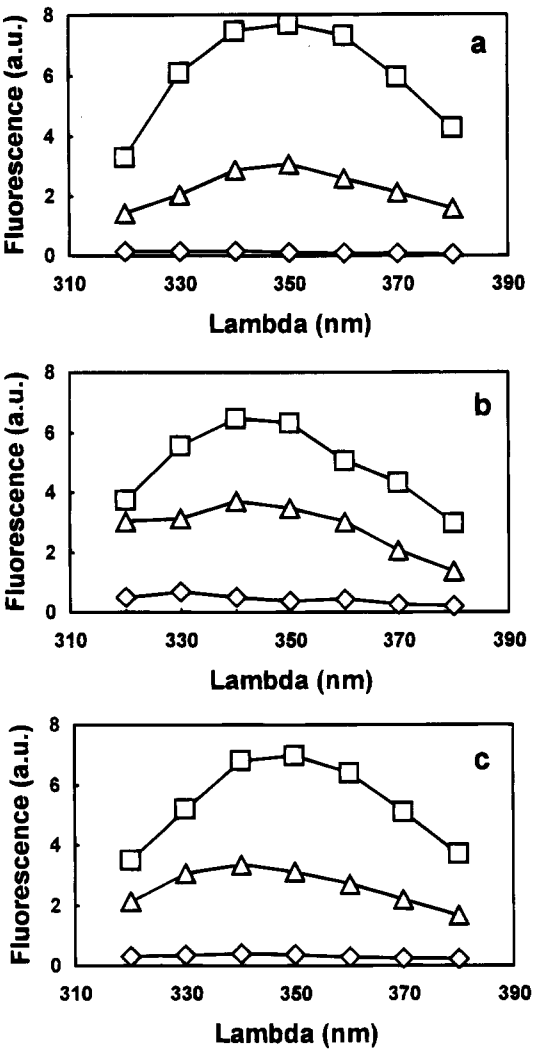

FIGURE 3: Spectra associated with the long component (squares), intermediate component (triangles), and short component (diamonds) of Trp-43 fluorescence intensity decay in F75 TetR free (a) and bound to the *tet* operator containing 76 bp fragment (b) and to sheared ct DNA (c). The spectra were normalized to have the same $\sum_i S_i$ where S_i is the area under the spectrum of component i. Measurements have been carried out in 10 mM Tris, pH 8.0, 5 mM NaCl, 10 mM βME, and 0.1 mM EDTA at a repressor dimer concentration of 1.1 μM. When present, the concentration of the *tet* operator was 1.5 μM, and that of nonspecific DNA was 90 μM (bp). In the presence of nonspecific DNA, 90% of the protein was bound to DNA.

indicating that the depolarization due to these motions was not complete. In the absence of DNA, the anisotropy at time 0, $r(t = 0)$, equal to $\sum_i r_i + r_\infty$, was about 0.20, a value clearly lower than 0.27, the limit anisotropy of Trp-43 at the same excitation and emission wavelengths (Chabbert et al., 1992). This clearly indicates the existence of an initial ultrafast rotational motion on the picosecond time scale that is not observable with our device. The initial anisotropy was not significantly altered upon F75 TetR binding to the *tet* operator containing 76 bp fragment. By contrast, it markedly increased to 0.24 upon binding to sheared ct DNA, due to a large increase in r_1, the amplitude of the 200-ps component. A similar increase was observed at different molar ratios of DNA to F75 TetR (not shown). This increase in $r(t = 0)$ indicates a decrease in the amplitude of the ultrafast rotational motions, which is not observed upon specific binding.

The motional processes on the picosecond−subnanosecond time scale are characterized by an order parameter S_f^2, calculated from the residual anisotropy remaining after depolarization by picosecond−subpicosecond motions:

$$S_f^2 = (r_2 + r_\infty)/r_0 \quad (9)$$

Using an r_0 of 0.27, we could determine an order parameter for the picosecond−subnanosecond motions of about 0.60 (Table 3). At the precision of our measurements, we did not observe significant changes in this order parameter upon binding. Using the wobbling in a cone model (Lipari & Szabo, 1980), this order parameter corresponds to a semiangle of 33−35°. Such an order parameter is expected for a Trp residue exposed to solvent as in free F75 TetR, but is surprisingly large for a residue at the interface with DNA. A similar behavior, however, has been observed for Trp-61 of mutant W61 TF1 protein which is located within one of the DNA grooves in the complex with DNA (Härd et al., 1988). These data indicate that *fluorescent* Trp residues (see Discussion) are not rotationally constrained but have intramolecular mobility within the complexes.

In the absence of DNA, the longest rotational correlation time was clearly lower than 20 ns, the overall rotational correlation time of the repressor dimer. It is difficult to assign it to a particular physical mode of motion, but it is probably related to segmental motions of the HTH motif involving a larger part of the protein. This rotational correlation time increased from 4.0 ns in the absence of DNA to 5.6 ns in both binding modes. If it is assumed that the fast motions are independent of the slow motions, the overall order parameter S^2, equal to r_∞/r_0, can be decomposed as (Clore et al., 1990):

$$S^2 = S_f^2 S_s^2 \quad (10)$$

where S_s^2 is the order parameter of the slow motions. This order parameter increased from 0.19 in the absence of DNA to 0.25 upon nonspecific binding and 0.36 upon specific binding, indicating a significant restriction of the amplitude of these motions. These values correspond to the wobbling in a cone whose semiangle decreased from 56° for free F75 TetR to 45° in the specific complex. These increases in the nanosecond rotational correlation time and in the related order parameter upon binding probably reflect tightening of segmental motions within the complexes.

DISCUSSION

Static Quenching of Trp-43 upon DNA Binding. The decrease in Trp-43 fluorescence intensity upon F75 TetR binding to specific or nonspecific DNA is not accounted for by the decrease in the average lifetime (Table 1). This is particularly evident for the specific complex for which the quenching, Q, calculated from the ratio of the average lifetimes ($Q = 0.34$) is considerably less than that calculated from the ratio of the steady-state fluorescence intensities ($Q = 0.72$). This cannot be accounted for by changes in the extinction coefficient of Trp-43 at the excitation wavelength, as the identity of the excitation spectra of Trp-43 in the unbound and bound states (see Results) rules out large amplitude changes in the absorption spectrum of *fluorescent* tryptophan (see below) upon binding. These absorption

Table 3: Fluorescence Anisotropy Parameters of Trp-43[a]

conditions	r	ϕ (ns)	θ_1 (ns)	r_1	θ_2 (ns)	r_2	r_∞	S_f^2	S_s^2
	0.082 ± 0.008	2.2 ± 0.2	0.18 ± 0.05	0.043 ± 0.010	4.0 ± 0.3	0.130 ± 0.005	0.030 ± 0.003	0.59 ± 0.03	0.19 ± 0.02
+sp DNA	0.110 ± 0.010	3.0 ± 0.2	0.18 ± 0.04	0.055 ± 0.010	5.6 ± 0.8	0.104 ± 0.006	0.056 ± 0.006	0.59 ± 0.04	0.36 ± 0.04
+nonsp DNA	0.106 ± 0.009	2.9 ± 0.2	0.20 ± 0.04	0.092 ± 0.005	5.6 ± 0.6	0.113 ± 0.006	0.038 ± 0.005	0.56 ± 0.04	0.25 ± 0.04

[a] Measurements have been carried out as described under Materials and Methods in 10 mM Tris, pH 8.0, 5 mM NaCl, 10 mM βME, and 0.1 mM EDTA. The emission wavelength was 350 nm. The F75 TetR dimer concentration was 1.4 μM. When the *tet* operator containing 76 bp fragment was present, the molar ratio of operator to repressor dimer was 1.4. When sheared ct DNA was present, its concentration was 160 μM, which corresponds to 94% of protein bound to DNA. The time-resolved anisotropy data correspond to the means ($\pm$ standard errors) of at least 10 measurements on the same sample. S_f^2 and S_s^2 are the order parameters of the fast (subnanosecond) and slow (nanosecond) motions.

spectra could not be determined directly due to absorption of DNA bases.

This apparent discrepancy clearly indicates that a fraction of the tryptophan residues is statically quenched upon binding. Our results support the notion that, in either complex, there is an equilibrium between (at least) two structurally distinct classes of tryptophan residues. Trp-43 in the first class is dynamically quenched and remains fluorescent, whereas Trp-43 in the second class is statically quenched and nonfluorescent. The degree of static quenching, i.e., the relative amount of nonfluorescent tryptophan residues, ω, equal to $1 - (F/F_0)(\bar{\tau}_0/\bar{\tau})$, increased from 0.20 $\pm$ 0.03 for the nonspecific complex to 0.57 $\pm$ 0.03 for the specific complex. The equilibrium constant K between nonfluorescent and fluorescent tryptophan residues, given by $\omega/(1 - \omega)$, increased from 0.25 $\pm$ 0.05 for the nonspecific complex to 1.32 $\pm$ 0.20 for the specific complex. This clearly demonstrates that static quenching of Trp-43 is favored in the complex with the *tet* operator DNA as compared to the complex with nonspecific DNA. The addition of 100 mM NaCl to the specific complex does not significantly alter the equilibrium constant K (1.38 $\pm$ 0.20).

Static quenching of tryptophan by DNA bases has been attributed to stacking interactions between the indole moiety and the nucleic acid bases [for reviews, see Hélène and Maurizot (1981) and Hélène and Lancelot (1982)]. Mutagenesis experiments have clearly shown the need of an aromatic residue (Phe or Tyr) or of His at position 43 (Baumeister et al., 1992), which are the amino acids for which stacking interactions are possible (Kumar & Govil, 1984). A molecular graphics model of the Tet repressor–*tet* operator complex based on the conventional HTH structure (Baumeister et al., 1992) shows that Trp-43 is located very close to the edges of base pairs 5 and 6 where it could be involved in stacking interactions with DNA bases. Our results strongly support this assumption. It has to be pointed out that the term "stacking" refers to the interaction between the π orbitals of two aromatic rings separated by van der Waals distances. Calculated optimized geometries of the stacked complexes between aromatic amino acids and base pairs show that the aromatic moieties overlap only partially (Kumar & Govil, 1984). Therefore, stacking implies that Trp-43 is in van der Waals contact with DNA bases, but it does not require intercalation of the indole moiety between two bases.

Thermodynamic calculations based on a two-step model (Scheme 1) similar to that proposed by Hélène and coworkers for the binding of short oligopeptides containing basic residues and tryptophan to nucleic acids (Brun et al., 1975; Montenay-Garestier et al., 1983; Rajeswari et al., 1987), in which Trp-43 does not interact with DNA in complex 1 and is involved in stacking interactions with DNA

Scheme 1

$$\text{TetR} + \text{DNA} \rightleftarrows \text{complex 1} \rightleftarrows \text{complex 2}$$

bases in complex 2, suggest that stacking might lead to a gain in free energy, $-RT \ln(1 + K)$, which would increase from about -0.5 kJ/mol in the nonspecific complex to about -2 kJ/mol in the specific complex. The gain in free energy per correctly formed protein-to-nucleic acid hydrogen bonds is estimated to be of the order of -0.5 kJ/mol (von Hippel & Berg, 1986). This suggests that stacking interactions might be involved in stabilizing the complex. The differential degree of static quenching between specific and nonspecific complexes suggests that Trp-43 stacking might contribute to the specificity of TetR binding, due either to a base sequence discrimination mechanism (Rajeswary et al., 1987) or to an effect on the DNA structure (Gabbay et al., 1976). Stacking of Trp-43 might participate in the deformation of *tet* operator DNA upon TetR binding (Tovar & Hillen, 1989; Niederweis, Wagenhofer, and Hillen, unpublished results). Although TetR is the only known HTH motif with a Trp residue at position 17, the presence of an aromatic residue (Tyr or Phe) or of a histidine at that position is not exceptional [e.g., NifA, MerR, P2 C, PurR, AraC, MetR (Dodd & Egan, 1990)], suggesting that stacking interactions might occur in other specific DNA-binding proteins.

Spectroscopic Properties of Fluorescent Trp-43 upon DNA Binding. The *fluorescence observed* in both complexes corresponds to Trp-43 residues which are *not* statically quenched upon DNA binding. The main difference in the spectroscopic properties of *fluorescent* tryptophans in both types of complexes is the emission maximum, which is 6 nm blue-shifted in the specific as compared to the nonspecific complex (Table 1). Shifts in emission maximum are usually interpreted as differential accessibility of the Trp residue to solvent (Burstein et al., 1973). This is not consistent with the acrylamide quenching data. The striking similarity in the dynamic quenching rates in both complexes (Table 1) implies a similar accessibility to solvent. This suggests that the shift might be related to the peculiar environment of Trp-43 in the specific complex. Specific recognition of a DNA sequence is usually achieved through hydrogen bonding (von Hippel & Berg, 1986). Involvement of polar groups in hydrogen bonding in the vicinity of Trp-43 is expected to reduce the amount of dipoles able to relax around the Trp excited state and, thus, the Stoke shift of the fluorescence emission.

The multiexponential decay of most single tryptophan proteins [for a review, see Beechem and Brand (1985)] is usually interpreted as related to the existence of different Trp rotamers or of multiple local environments of Trp due to protein heterogeneity. Both the lifetimes and the relative

amplitudes of the three components of Trp-43 fluorescence decay in free F75 TetR correlate well with those observed for Trp residues in model α-helices (Willis et al., 1994). This suggests that, as for these model systems, the three decay times might correspond to the three ground-state χ^1 rotamers of the tryptophan residue. As Trp-43 is located at the interface with DNA, packing requirements upon binding might constrain the Trp side chain and affect rotamer frequencies. The similarity in Trp-43 decay parameters in the specific and nonspecific complexes suggests that the steric constraints are similar in both types of complexes. The marginal changes in the lifetimes upon binding suggest that the vicinity of DNA does not add efficient deactivation pathways and that the quencher groups or energy acceptors within the protein matrix are not markedly altered upon binding.

Bajzer and Prendergast (1993) have recently presented an alternative multiexponential model in which deexcitation of the excited fluorophore occurs mainly through transfer of energy mechanisms. The presence of nucleic acids in the vicinity of Trp-43 is expected to add deexcitation by "transfer of energy " mechanisms, as fluorescence resonance energy transfer or electron transfer from indole to purine and pyrimidine bases (Hélène & Lancelot, 1982). In view of this model, the apparent changes in the preexponential factors might reflect these additional deexcitation pathways. Irrespective of the physical interpretation of the observed fluorescence decay components, the striking similarity in the decay parameters of Trp-43 upon F75 TetR binding to either specific or nonspecific DNA is consistent with the assumption that the photophysical origin of the changes in the fluorescence decay as compared to free F75 TetR is the same in both complexes.

Acrylamide quenching (Table 1) and anisotropy data (Table 3) suggest that *fluorescent* Trp-43 is in an environment less constrained and more accessible to solvent than in the molecular graphics model of the Tet repressor–*tet* operator interaction (Baumeister et al., 1992). On the other hand, this model is consistent with stacking interactions between Trp-43 and DNA bases. The present study does not allow us to better characterize the fluorescent and nonfluorescent Trp-43 classes and the nature of the conformational changes between them. The main spectroscopic difference between the specific and nonspecific complexes is the preferential static quenching observed upon *tet* operator binding. The presence of a dominant static quenching process upon specific binding supports the assumption that stacking interactions are involved in the complex between TetR and its operator.

ACKNOWLEDGMENT

We thank Dr. M. Takahashi (Paris, France) for providing us with the programs for nonspecific DNA binding data analysis.

REFERENCES

Bajzer, Z., & Prendergast, F. (1993) *Biophys. J. 65*, 2313–2323.
Ballini, J. P., Vigny, P., & Daniels, M. (1983) *Biophys. Chem. 18*, 61–65.
Baumeister, R., Helb, V., & Hillen, W. (1992) *J. Mol. Biol. 226*, 1257–1270.
Beck, C. G., Mutzel, R., Barbe, J., & Muller, W. (1982) *J. Bacteriol. 150*, 663–643.
Beechem, J. M., & Brand, L. (1985) *Annu. Rev. Biochem. 54*, 43–71.
Bertrand, K. P., Postle, K., Wray, L. V., Jr., & Reznikoff, W. S. (1983) *Gene 23*, 149–156.
Brun, F., Toulmé, J.-J., & Hélène, C. (1975) *Biochemistry 14*, 558–563.
Burstein, E. A., Vedenkina, N. S., & Ivkova, M. N. (1973) *Photochem. Photobiol. 18*, 263–279.
Chabbert, M., Hillen, W., Hansen, D., Takahashi, M., & Bousquet, J. A. (1992) *Biochemistry 31*, 1951–1960.
Clore, G. M., Szabo, A., Bax, A., Kay, L. E., Driscoll, P. C., & Gronenborn, A. M. (1990) *J. Am. Chem. Soc. 112*, 4989–4991.
Cross, A. J., & Fleming, G. R. (1984) *Biophys. J. 46*, 45–56.
Daniels, M., & Hauswirth, W. (1971) *Science 171*, 675–677.
Dodd, I. B., & Egan, J. B. (1990) *Nucleic Acids Res. 18*, 5019–5026.
Eftink, M. R., & Ghiron, C. A. (1976) *Biochemistry 15*, 672–680.
Ettner, N., & Jacob, L. (1993) *Merck Spectrum 1*, 24–26.
Freemont, P. S., Lane, A. N., & Sanderson, M. R. (1991) *Biochem. J. 278*, 1–23.
Gabbay, E. J., Adawadhhkar, L., Kapicak, S. P., & Wilson, W. D. (1976) *Biochemistry 15*, 152–157.
Hansen, D., & Hillen, W. (1987) *J. Biol. Chem. 262*, 12269–12274.
Härd, T., Hsu, V., Sayre, M. H., Geiduschek, E. P., Appelt, K., & Kearns, D. (1989) *Biochemistry 28*, 396–406.
Harrison, S. C., & Aggarwal, A. K. (1990) *Annu. Rev. Biochem. 59*, 933–969.
Hélène, C., & Maurizot, J. C. (1981) *CRC Crit. Rev. Biochem.10*, 213–258.
Hélène, C., & Lancelot, G. (1982) *Prog. Biophys. Mol. Biol. 39*, 1–68.
Hillen, W., Schollmeier, K., & Gatz, C. (1984) *J. Mol. Biol. 172*, 185–201.
Hinrichs, W., Kisker, C., Duvel, M., Muller, A., Tovar, K., Hillen, W., & Saenger, W. (1994) *Science 264*, 418–420.
Kleinschmidt, C., Tovar, K., Hillen, W., & Porschke, D. (1988) *Biochemistry 27*, 1094–1104.
Kumar, N. V., & Govil, G. (1984) *Biopolymers 23*, 2009–2024.
Lakowicz, J. R. (1983) in *Principles of Fluorescence Spectroscopy*, pp 111–153, Plenum Press, New York.
Lami, H., & Piémont, E. (1992) *Chem. Phys. 163*, 149–159.
Lipari, G., & Szabo, A. (1980) *Biophys. J. 30*, 489–506.
McGhee, J. D., & von Hippel, P. H. (1974) *J. Mol. Biol. 86*, 469–489.
Montenay-Garestier, T., Takasugi, M., & Le Doan, T. (1983) in *Nucleic Acids: The Vectors of Life* (Pullman, B., & Jortner, J., Eds.) pp 305–315, Reidel, Dordrecht, The Netherlands.
Pabo, C. O., & Sauer, R. T. (1992) *Annu. Rev. Biochem. 61*, 1053–1095.
Rajeswari, M. R., Montenay-Garestier, T., & Hélène, C. (1987) *Biochemistry 26*, 6825–6831.
Steiz, T. A. (1990) *Q. Rev. Biophys. 23*, 205–280.
Takahashi, M., Sakumi, K., & Sekiguschi, M. (1990) *Biochemistry 29*, 3431–3436.
Tovar, K., & Hillen, W. (1989) *Nucleic Acids Res. 17*, 6515–6522.
Vix, A., & Lami, H. (1995) *Biophys. J. 68*, 1145–1151.
Von Hippel, P. H., & Berg, O. G. (1986) *Proc. Natl. Acad. Sci. U.S.A. 83*, 1608–1612.
Wahl, P., & Auchet, J. C. (1972) *Biochim. Biophys. Acta 285*, 99–117.
Werner, T. C., & Forster, L. S. (1979) *Photochem. Photobiol. 29*, 905–909.
Willis, K. J., Neugebauer, W., Sikorska, M., & Szabo, A. G. (1994) *Biophys. J. 66*, 1623–1630.
Wissmann, A., Baumeister, R., Muller, G., Hecht, B., Helbl, V., Pfleiderer, K., & Hillen, W. (1991) *EMBO J. 10*, 4145–4152.

BI9502755